Synthesis and characterization of mesoporous silica films encapsulating titanium dioxide particles Photodegradation of 2,4-dichlorophenol

William A. Adams [a], Martin G. Bakker [a,*], Transito Macias [b], I. Atly Jefcoat [b]

[a] *Department of Chemistry, The University of Alabama, Tuscaloosa, AL 35487-0336, USA*
[b] *Dave C. Swalm School of Chemical Engineering, Mississippi State University, Starkville, MS 39762, USA*

Abstract

Degussa P-25 TiO_2 encapsulated in a SBA-15 mesoporous thin film silica matrix prepared using a block copolymer templating method. The film structure was characterized using small angle X-ray diffraction (XRD), variable angle spectroscopic ellipsometry (VASE), and polarized light microscopy. The photoactivity of the films was assessed using HPLC and UV–vis spectroscopy to study the photodegradation of 2,4-dichlorophenol, an industrial pollutant, in water under 350 nm irradiation. The unoptimized film was found to be approximately half as photoactive as an equivalent dispersion of TiO_2.
© 2004 Elsevier B.V. All rights reserved.

1. Introduction

There has been considerable interest in the use of TiO_2 semiconductor particles as a means to degrade organic wastes [1,2]. The bandgap of TiO_2 is above 3.0–3.2 eV, which corresponds to a wavelength of approximately 380–400 nm. Therefore, wavelengths below 380 nm allow for the excitation of electrons in the valence band of the semiconductor to the conduction band. This produces electron-hole pairs that act as oxidizing and reducing agents. Decomposition of surface bound molecules can occur by electron transfer from the TiO_2 particles to adsorbed organic species or reaction with hydroxyl radicals produced by the decomposition of water. Degussa P-25 TiO_2 is an active form of TiO_2 that is often used as a standard titanium dioxide photocatalyst due to its high activity. This activity has been linked to the presence of both rutile and anatase crystals present in the P-25 TiO_2 [3].

Much of the research in semiconductor photodecomposition has focused on the application of aqueous TiO_2 dis-persions, or slurries, for photodegradation of organic compounds [4–6]. The application of TiO_2 particles as a means of waste disposal has drawbacks associated with the colloidal nature of the small particles. Such colloids suspend in water and present a problem for real world applications because it is necessary to filter and separate the particles from the aqueous phase. This can be time consuming and expensive. An alternative method that has been explored is the use of permeable TiO_2 membranes [7,8]. In another approach, the TiO_2 particles were supported on silica [9–11]. Recently, the development of templated methods of synthesizing mesoporous materials with ordered arrays of pores with a narrow pore size between 2 and 10 nm, has raised the prospect of superior photocatalysts [12] and more efficient supports for TiO_2 particles [10,13–15]. In these systems, the TiO_2 particles are confined to the surface of the support, which limits the overall density obtainable and also has the potential for significant particle loss since the particles are not covalently bonded to the support. There is therefore interest in novel methods of incorporating TiO_2 particles into porous supports. Recent research has focused on postsynthesis methods of growing titanium dioxide within mesoporous silica [16]. At high loading, the titanium forms photoactive TiO_2. However, this form of TiO_2 is anatase,

* Corresponding author. Tel.: +1 205 348 9116; fax: +1 205 348 9104.
E-mail address: bakker@bama.ua.edu (M.G. Bakker).

which gives lower photoactivity than, for example, P-25 TiO_2. It is not clear that any of the methods for making mesoporous TiO_2 or incorporating TiO_2 within mesoporous silica have photoactivity comparable to the most photoactive forms of TiO_2. We were therefore interested in determining if incorporating the TiO_2 particles within the bulk mesoporous silica, i.e. encapsulation, would produce a more efficient media. P-25 TiO_2 has a particle size of 12–20 nm, compared to the 2–10 nm diameter that is typical for mesopores. Therefore, particles would become encapsulated and not be able to escape through the pores present in the silica matrix. The encapsulation, would therefore be expected to give lower loss of TiO_2 particles, potentially would give higher TiO_2 density, controllable diffusion properties (through control of the pore size and ordering), and could give more efficient photodegradation as reported by Xu and Langford [14]. This approach also has the advantage that if new methods of synthesizing TiO_2 particles with superior properties to those of existing particles are developed, such new particles can be readily incorporated into our materials.

The SBA-15 [17,18] form of mesoporous silica is prepared by combining a source of silica (SiO_x) such as a silicon alkoxide with a block copolymer which acts as the template for the formation of pores. The silicon alkoxide undergoes hydrolysis to produce silicic acid and polymers of silicic acid. At low pH, condensation will occur at a slow rate, which gives time for the polymer to aggregate and self organize into hydrophobic and hydrophilic domains. The silicate polymers solubilize in the hydrophilic domains where they condense. After the condensation reaction is complete, the template can be removed to leave porous silica. Thin films of mesoporous silica can be made by adding appropriate solvents to the silicate/polymer solution to aid in spreading the mixture and to slow the silicate condensation. If appropriate shear forces are applied during the film preparation, then complete or partial alignment of the pores parallel to the surface can be produced [17]. The benefits of thin film templated silica include large pores for faster diffusion, parallel orientation to the surface to allow for an enhanced contact time, and porous walls to allow for diffusion perpendicular to the surface.

This work focuses on the characterization of a composite of Degussa P-25 TiO_2 within an SBA-15 mesoporous thin film matrix. Recent research has focused on the application of TiO_2 photocatalysts for the degradation of chlorinated organic wastes, since these compounds are hazardous and widely produced in industry [4,5,12,19]. This work examines the qualitative and quantitative aspects of 2,4-dichlorophenol degradation occurring within small scale reactors containing SBA-15/P-25 thin films and compares the results to that obtained from slurries of P-25 TiO_2. Time dependence of irradiation and the effect of varying the amount of TiO_2 are also examined.

2. Experimental

2.1. Materials

For the SBA-15 synthesis, tetraethyl orthosilicate (TEOS, 98% Aldrich), poly(ethylene oxide)–poly(propylene oxide)–poly(ethylene oxide) block copolymer (Pluronic P123, BASF), and P-25 titanium dioxide (Degussa) were used as received. Concentrated HCl (Fisher) in deionized water (pH 1–2) and 100% ethanol (Fisher) were available.

The 2,4-dichlorophenol was obtained from Aldrich and used as received, as HPLC analysis did not show the presence of any impurities prior to irradiation.

2.2. Instrumentation

X-ray diffraction (XRD) data was collected on a Rigaku D/MAX-2BX Horizontal XRD Thin Film Diffractometer using Cu Kα radiation ($\lambda = 1.5406$ Å). A variable angle spectroscopic diffractometer from J.A Woollam Co. Inc. was used in mesoporous silica film characterization. The instrument used an HS-190 75 W monochrometer with a VB-250 control module. Data was analyzed using the WVASE 32 software. All samples were coated onto silicon wafers for analysis.

UV–vis spectra were determined using a Cary 50 scan UV–vis spectrophotometer. The blank used for all samples was water. HPLC was performed on an Agilent 1100 series High Performance Liquid Chromatograph with autosampler using EPA Method 604 Phenols by HPLC and a Symmetry C_8 5 μm 3.9 mm × 150 mm column. All other parameters were as specified by the EPA method. A UV detector was used at a wavelength of 280 nm.

The irradiator used was a Rayonet Irradiator that contained 350 nm Hg lamps. Inside the irradiator, a magnetic stirrer was used to stir samples during irradiations.

2.3. Synthesis of SBA-15/P-25 thin films

The procedure of Alberius et al. was used [17]. First, 10.4 g tetraethyl orthosilicate (TEOS) was combined with 5.0 g pH 1–2 water and 12.0 g 100% ethanol. This solution was sealed with parafilm and allowed to stir for 20 min. A separate solution was prepared containing the poly(ethylene oxide)–poly(propylene oxide)–poly(ethylene oxide) block copolymer (Pluronic P123) in 8.0 g 100% ethanol and was sealed and stirred until the P123 was completely dissolved, typically 30 min. The two solutions were combined and allowed to stir for 3 h. Samples that were to contain TiO_2 were prepared by mixing the two solutions as before, but then adding TiO_2 and stirring for 3 h, for example, adding 0.420 g TiO_2 to give a final film containing 12.5 wt.% P-25 TiO_2. After the 3 h, a dip-coater was used to coat the material onto the substrate of choice to form a thin film. The dip-coater wheel rotates at 0.5 rpm and coated the substrate at a speed of 1 mm/s. The films were then air

dried overnight. Typically these films were replicated in quadruplicate.

2.4. Removal of template from silica thin films

All samples to the point before the removal of templating polymer will be referred to as "as prepared" samples. Two methods of template removal were tested. The first involved an ethanol wash in which the film was suspended in a beaker of 100% ethanol and stirred overnight. The sample was then washed once with deionized water and air dried.

The second method involved heating the thin film to high temperatures using a programmable oven and a specified temperature ramping program. The program consisted of heating the sample from 50 °C to 400 °C at 1 °C/min. The temperature was held at 400 °C for 240 min, and then the cooling program allowed the sample to return to room temperature by reducing the heat at 1 °C/min. Following removal from the oven, the samples were washed in deionized water and allowed to dry overnight. Dip-coated tubes showed an even coating of film on both the inside and outside surfaces of the glass. The coating was an opaque white film.

2.5. Irradiated samples

All irradiations were performed using a Rayonet Irradiator with 350 nm high pressure Hg lamps. The flux for the irradiator was found to be 4.84×10^{14} photons/s, which was the flux incident on the vials used in analysis. This calculation was based on the known quantum efficiency of the photochemical reaction of potassium ferrioxalate [20]. For the thin film analysis, 8 mL of 55 ppm 2,4-dichlorophenol solution and a 2-in. long, 11 mm diameter glass tube dip-coated with a thin film of SBA-15/P-25 were placed inside a 10 mL Pyrex vial. The coated glass tube was held in place by a small rubber stopper that also sealed the reactor. A small stir bar was used to stir the solution during irradiation. The irradiated solution was then analyzed using HPLC and/or UV–vis spectrophotometer.

3. Results and discussion

3.1. Characterization

3.1.1. XRD

The presence of an ordered structure was established by small angle X-ray diffraction. SBA-15 gives characteristic peaks [17] in the small angle, 0–5°, region of a $\theta/2\theta$ XRD scan. These peaks are representative of the various crystal lattice planes ([1 0 0], [2 0 0], [3 0 0], etc.) that diffract the X-rays. The presence of these specific crystal lattice planes indicates that the material is ordered. Typically, the higher the order of diffraction, the weaker is the diffracted intensity.

All initial films prepared by using the SBA-15 silica method were analyzed by XRD. Each sample showed an
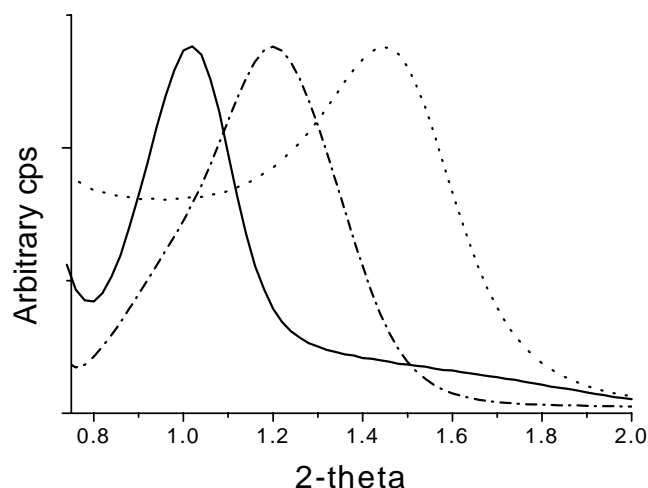

Fig. 1. X-ray Diffraction data of an as prepared SBA-15 silica thin film, an ethanol washed SBA-15 silica thin film, and a calcined SBA-15 silica thin film ((—) as prepared, (–·–) EtOH wash, (. . .) calcined).

intense peak at 0°, which is due to the direct beam of the X-ray source. For the "as prepared" samples, a [1 0 0] lattice peak, which is characteristic of ordered samples, can be seen at about 1.0° as shown in Fig. 1. This angle corresponds to a d-spacing of 9.2 nm and a spacing from pore center to pore center of 10.6 nm, and matches the spacing expected for SBA-15 grown by this method [17].

Spectra were also taken of samples that had undergone washes and calcination in order to remove the templating material. It is known that when the template is removed, the mesoporous silica film shrinks perpendicular to the surface [17]. This would be seen in the XRD spectra as a shift of the peaks to a higher angle. As can be seen in Fig. 1, the "as prepared" sample contains peaks at smaller angles than the ethanol washed sample. Similarly, the ethanol washed sample contains peaks at smaller angles than in the calcined sample. In the washed sample, the [1 0 0] peak appears at 1.2°, corresponding to a 9.0 nm pore spacing, and the calcined sample appears at 1.45°, or 7.7 nm pore spacing. This suggests that the template may not be completely removed in the ethanol washed sample. Therefore, since the calcined sample has the smallest lattice spacing, it is believed to contain the least template, suggesting it should have most accessible pores. This would be expected to give better diffusion. The pore diameter can be estimated using the lattice spacing and density, 46%, of the film determined by the VASE measurements (below). For a film thickness of 378 nm [vid infra], the average pore diameter for the calcined sample was approximately 2–3 nm based on geometrical calculations.

3.1.2. Variable angle spectroscopic ellipsometry (VASE)

Further characterization of the films was performed by variable angle spectroscopic ellipsometry (VASE) in which the film thickness and void space were determined based on the refraction of polarized light within the sample and the optical constants of the material. The analysis of the
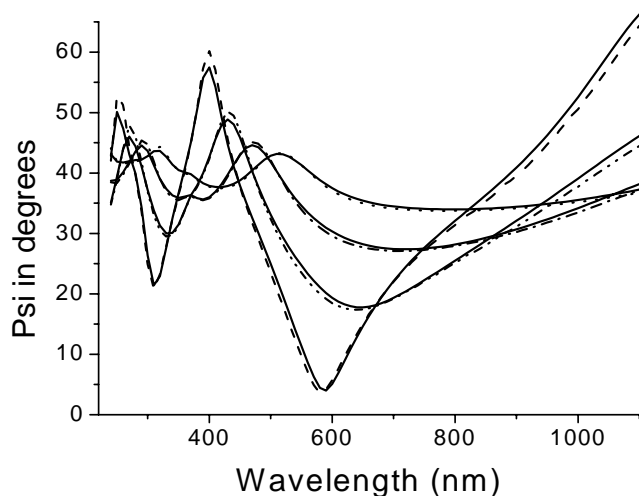
Fig. 2. Variable Angle Spectroscopic Ellipsometry spectrum of a calcined SBA-15 silica thin film. Spectrum contains four angles used for data analysis and four angles used for model calculation ((—) models, (...) 45°, (–··–) 55°, (–··) 65°, (––––) 75°).

VASE data involved fitting a model to the experimental data. Adjustable parameters include film thickness, composition, and interfacial roughness. The porous nature of the silica necessitates the use of an effective medium approximation (EMA). With an EMA, the software fits the relative amounts of the two components, silica and air. The wavelength of light is 240 nm–1100 nm, much longer than the 7.7 nm repeat pore spacing observed with the mesoporous structure. What is observed will therefore be a weighted average of the silica walls and the empty pores. The sample films were prepared on a silicon wafer. Glass substrates were not used since the samples were silica, and it would be more difficult to differentiate between the substrate and the sample.

VASE was performed on calcined SBA-15 films in order to determine the thickness of the film and to understand the distribution of the pore space within the silica. Fig. 2 shows the spectrum obtained by the ellipsometer and the fits generated by the model. Four angles were used (45°, 55°, 65°, and 75°) in order to constrain the parameters. The results of the fit for a calcined mesoporous silica film showed a film thickness of 378 nm and a void space of 46.6%. The mean square error of 17.2 associated with the fit was acceptable.

3.2. Polarized microscope images

Images were taken of calcined SBA-15/P-25 thin films on microscope slides. Images of a 10 wt.% P-25 sample at a magnification of 5X and 50X in an SBA-15 thin film matrix can be seen in Fig. 3. TiO$_2$ particles can be clearly seen as dark spots. The magnification of 50X shows that the TiO$_2$ particles appear to be clumping together. Films which contain clumped TiO$_2$ would be expected to be less photoactive since the photolysis occurs at the surface of the TiO$_2$ and clumping would reduce available surface area. Therefore, it
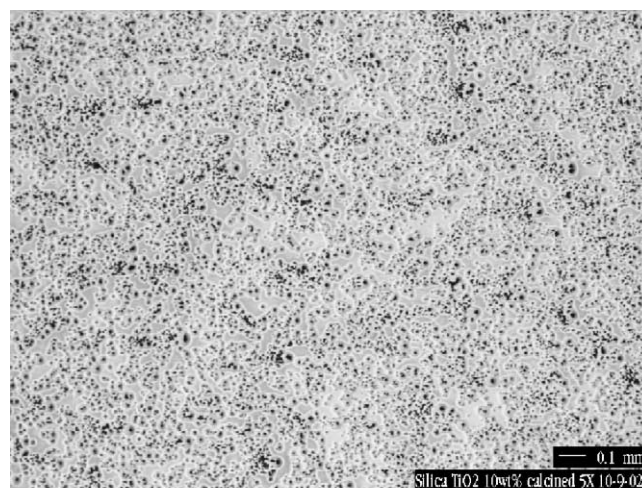
(a)
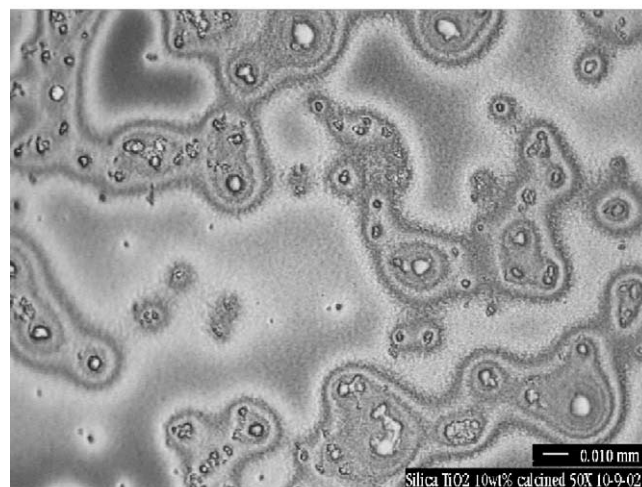
(b)

Fig. 3. Polarized microscope image of SBA-15/P-25 thin film. Images are shown at (a) 5X and (b) 50X.

may be desirable to prevent this aggregation from occurring to maximize the efficiency of photodegradation.

3.3. Photolysis of 2,4-dichlorophenol using SBA-15/P-25 thin film tubes

The photoactivity of the SBA-15/P-25 films was assessed by examining the photodecomposition of 2,4-dichlorophenol (2,4-DCP) over time. HPLC was used to determine the concentration of 2,4-DCP. The amount of 2,4-DCP remaining as a function of irradiation time is shown in Fig. 4. By 2.5 h irradiation, all of the 2,4-DCP has been removed. In order to determine if the loss of 2,4-DCP by mechanisms other than decomposition by TiO$_2$ were important, two other experiments were carried out. Samples of 2,4-DCP irradiated for 3 h without tubes exhibit about 27% degradation as determined by HPLC. This would be expected since 2,4-DCP absorbs light at 350 nm and is known to photodegrade. Samples
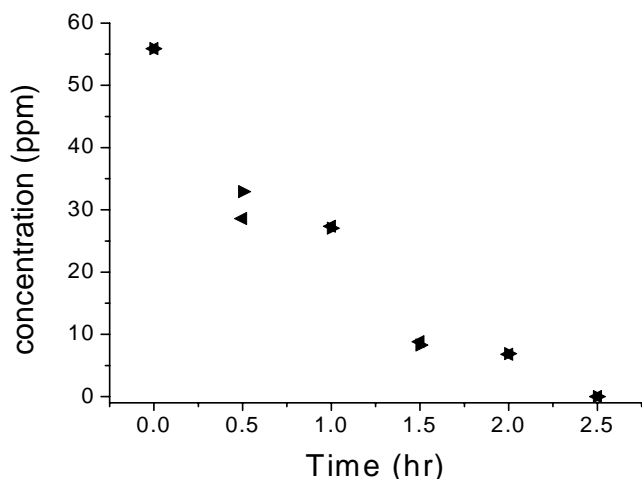
Fig. 4. Graph showing the concentration of 2,4-DCP over a period of irradiation times. Concentrations determined by HPLC((◄) tube 1; (►) tube 2).
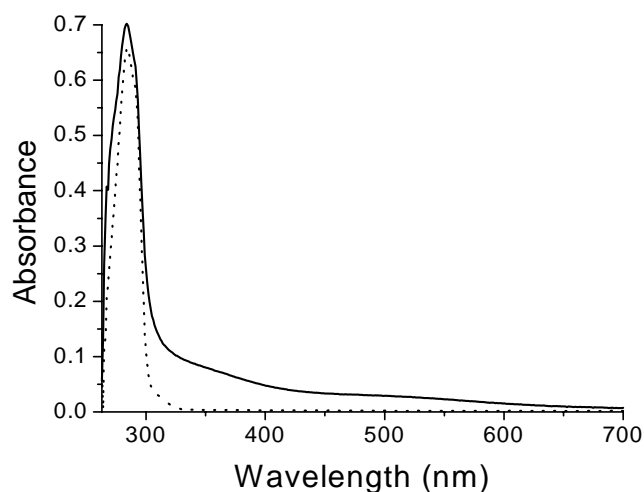

Fig. 5. UV–vis spectra of a standard 55 ppm 2,4-DCP solution and a standard 55 ppm DCP solution after a 1 h stirred irradiation in the small scale reactor containing an SBA-15/P-25 thin film tube((—) thin film coated tube in solution, (...) 2,4-DCP standard).

stirred in the dark for 3 h in the presence of tubes only show about 4% loss of sample. This could be due to adsorption of the 2,4-DCP to the silica tubes. Therefore, photodegradation on the TiO$_2$ thin films on the tubes is the dominant degradation mechanism.

Although Fig. 4 shows that at 2.5 h all of the 2,4-DCP has been degraded, the chromatographs from HPLC also showed the presence of compounds at shorter retention times. Since a non-polar column was used, these compounds must be less hydrophobic degradation products produced from the degradation of the 2,4-DCP.

Based on HPLC results, the 2,4-DCP concentration after irradiation of the 1 h sample was 48.3% of the original concentration. The formation of degradation products is not only visible in the chromatographs, but is also clearly visible in the UV–vis spectra. Analysis of a 55 ppm 2,4-DCP standard shows a strong absorption in the UV range at 284 nm, as seen in Fig. 5. The effect of irradiation in the presence of SBA-15/P-25 thin film can be clearly seen in Fig. 5. This spectrum showed a trend present in all irradiated samples. The irradiated samples cannot be directly compared to standard samples due to absorption by other species. It is believed that these are 2,4-DCP photodegradation products. These degradation products had absorptions which extended into the visible range of the spectrum, which often led to the production of lightly colored solutions.

An averaged set of spectra, shown in Fig. 6, was taken from the results of timed irradiations (0.5, 1.0, 1.5, 2.0, 2.5, 5.0, 7.5 h) of two SBA-15/P-25 coated tubes in the small scale reactors replicated in duplicate. These spectra showed an increase in absorbance at about 280 nm due to the production of degradation products. Further, absorbance peaks around 300 nm and 650 nm are observed for these products to indicate the presence of different types of degradation products. The observation of a number of products in the HPLC is consistent with the observation of absorbance

peaks at about 350 nm and around 510 nm. Within 5 h, all of the 2,4-DCP had been consumed. The early disappearance of the peak around 350 nm suggests that this peak is from a component formed directly from 2,4-DCP.

3.4. P-25 TiO$_2$ loading dependence in SBA-15/P-25 thin films

The effects of P-25 TiO$_2$ loading can be seen in Fig. 7. All samples shown underwent a 3 h stirred irradiation. The TiO$_2$ weight percentages present in the final films were 5.0, 12.5, 20.0, and 30.0 wt.%, where the balance is silica. The 5.0 wt.% sample showed a 2,4-DCP concentration of
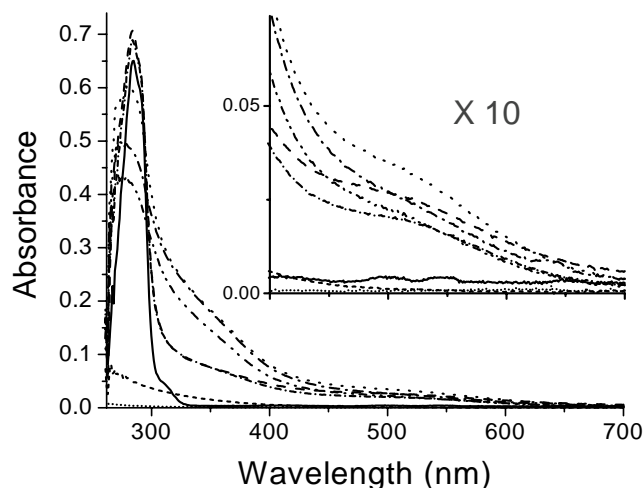

Fig. 6. Averaged UV–vis spectra of standard 2,4-DCP solutions after various timed stirred irradiations ((—·—··—) 0.5 h; (— —) 1.0 h; (...) 1.5 h; (—··—) 2.0 h; (—··) 2.5 h; (- - - -) 5.0 h; (...) 7.5 h, (—) 2,4-DCP std) in the small scale reactors using the same SBA-15/P-25 thin films tubes. Average is based on two replicates.
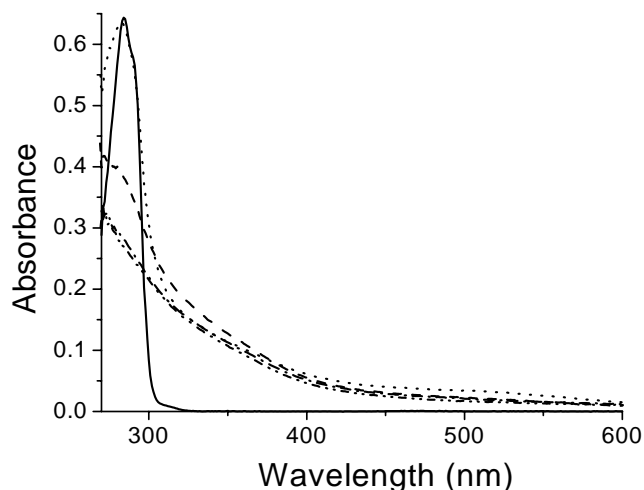
Fig. 7. UV–vis spectra of standard 2,4-DCP solutions after 3 h stirred irradiation using various loading weight percentages ((– –) 5.0 wt.%; (. . .) 12.5 wt.%; (–·–) 20.0 wt.%; (–··) 30.0 wt.%; (—) 2,4-DCP std) of P-25 TiO$_2$.

7.9 ppm after 3 h irradiation as determined by HPLC analysis. There was also the presence of degradation products, as indicated by the increase in absorption at 284 nm, and there was absorption due to degradation products around 500 nm. The 12.5 wt.% sample appeared to have an increase in degradation product production, and no 2,4-DCP was detected. Therefore, the 2,4-DCP must have been completely degraded, and the degradation products were probably beginning to undergo significant photolysis themselves. The results from the 20.0 wt.% and 30.0 wt.% samples showed that the samples still contained considerable degradation products, but no 2,4-DCP. However, the rate of removal of products was not very much faster than for the 12.5 wt.% sample. The degradation rates for the 20 wt.% and 30 wt.% were very similar. Initial studies of the 12.5 wt.% thin film showed that the film absorbed 92% of the UV light. The 20 wt.% and 30 wt.% samples could therefore absorb little extra light and so only a very modest increase in photodegradation compared to 12.5 wt.% would be expected.

3.5. Thin film photolysis versus photolysis of dispersions

The results from an analysis of the thin film experiments and the results from analysis of a dispersion were compared with each other. The dispersion consisted of 0.8 mg of P-25 TiO$_2$ mixed with the 2,4-DCP standard. This amount of TiO$_2$ was approximately the same amount of TiO$_2$ present in the 12.5 wt.% reactor tubes. HPLC analysis of the dispersion samples showed 14.2 ppm of 2,4-DCP remaining after 0.5 h irradiation, and the thin film samples showed 30.8 ppm of 2,4-DCP remaining after 0.5 h. This indicates that the thin film method was able to degrade the 2,4-DCP approximately half as fast as the dispersion method. However, the geometry and absorbance differed somewhat between the dispersions

and the films. The cross-sectional areas differed between films and dispersions by a factor of 1.1 (the dispersions having the larger cross-section). Further, the absorbance measured for the dispersions varied from 2 at the center of the vial to approximately 1 at the outside edge of the vial, compared to an absorbance of 0.7 for the film samples. The slurry samples therefore absorbed approximately 30% more light than the films samples, so that on a per photon basis, the film has approximately 2/3rds the efficiency of the comparable slurry samples. This is a reasonably favorable result, as the film has not yet been optimized in terms of thickness, pore size, and clumping. We have not yet carried out an analysis of the degradation products, but if the relative reactivity of 2,4-DCP and the degradation products are different in films and in dispersions, then this might allow for matrices to be optimized for one process rather than another. This could include the acceleration of one process and the suppression of another, e.g. dehalogenation, to allow for the recycling of some material. Further, pore size selectivity might have advantages in decomposing a small undesirable component of a mixture, in the presence of larger compounds. By encapsulating TiO$_2$ within mesoporous silica, it should be possible to optimize the two components separately, e.g. by incorporating more active TiO$_2$ particles [21]. We have already found that the use of the mesoporous silica films provides advantages in studying the photodecomposition of TiO$_2$ by eliminating the need to filter the solutions allowing for more efficient analysis.

4. Conclusions

As confirmed by XRD and VASE, the mesoporous silica films incorporating P-25 TiO$_2$ particles were prepared. It appeared that calcining the samples removed the most templating material. By using the 12.5 wt.% SBA-15/P-25 thin films, there was complete degradation of 2,4-DCP within 2.5 h of irradiation. Degradation product formation was evident within the first 0.5 h of irradiation. It also appeared that following 2,4-DCP degradation, the degradation products themselves undergo photolysis. According to UV–vis spectra, only trace amounts of degradation products were detectable after 7.5 h of irradiation. After 0.5 h of irradiation, the rate of degradation of the SBA-25/P-25 thin films was comparable with the rate of degradation with the dispersed TiO$_2$ samples.

Work is continuing with the characterization of the degradation products and studies of the kinetics of the photolysis. The photodegradation mechanisms of 2,4-DCP and other similar compounds are known in the literature [4–6,12,19], and the information will be applied for characterization. A more intensive comparison of degradation rates will be carried out between samples of SBA-15/P-25 thin films and P-25 dispersions. Also, film thickness differentiation will be explored to determine optimal parameters for the most efficient photolysis of organic compounds.

Acknowledgements

References

[1] N. Serpone, E. Pelizzetti, Photocatalysis: Fundamentals and Applications, Wiley, New York, 1989.

[2] M.R. Hoffmann, S.T. Martin, W. Choi, D.W. Bahnemann, Chem. Rev. 95 (1995) 69.

[3] D. Hurum, A.G. Agrios, K.A. Gray, T. Rajh, M.C. Thurnauer, J. Phys. Chem. B 107 (2003) 4545.

[4] G. Mills, M.R. Hoffmann, Environ. Sci. Technol. 27 (1993) 1681.

[5] A.B. Prevot, E. Pramauro, Talanta 48 (1999) 847.

[6] B. Pal, M. Sharon, J. Mol. Catal. A: Chem. 160 (2000) 453.

[7] J. Sebate, M.A. Anderson, H. Kikkawa, M. Edwards Jr., C.G. Hill, J. Catal. 127 (1991) 167.

[8] Q. Dai, Z. Zhang, N. He, P. Li, C. Yuan, Mater. Sci. Eng. C 8/9 (1999) 417.

[9] L.J. Alemany, M.A. Baneres, E. Pardo, F. Martin, M. Galan-Fereres, J.M. Blasco, Appl. Catal. B: Environ. 13 (1997) 289.

[10] Y. Xu, H. Langford, J. Phys. Chem. 99 (1995) 11501.

[11] S.W. Ahn, L. Kevan, J. Chem. Soc., Faraday Trans. 94 (1998) 3147.

[12] Q. Dai, N. He, K. Weng, B. Lin, Z. Lu, C. Yuan, J. Inclusion Phenom. Macrocycl. Chem. 35 (1999) 11.

[13] A.A. Belhekar, S.V. Awate, R. Anand, Catal. Commun. 3 (2002) 453.

[14] Y. Xu, C.H. Langford, J. Phys. Chem. B 101 (1997) 3115.

[15] Y. Hsien, C. Chang, Y. Chen, S. Cheng, Appl. Catal. B: Environ. 31 (2001) 241.

[16] Z. Luan, E.M. Maes, P.A.W. Van der Heide, D. Zhao, R.S. Czernuszewicz, L. Kevan, Chem. Mater. 11 (1999) 3680.

[17] P.C.A. Alberius, K.L. Frindell, R.C. Hayward, E.J. Krammer, G.D. Stucky, B.F. Chmelka, Chem. Mater. 14 (2002) 3284.

[18] D. Zhao, P. Yang, N. Melosh, J. Feng, B.F. Chmelka, G.D. Stucky, Adv. Mater. 10 (1998) 1380.

[19] D.G. Crosby, H.O. Tutass, J. Agric. Food Chem. 14 (1966) 596.

[20] C.G. Hatchard, C.A. Parker, Proc. R. Soc. A235 (1956) 518.

[21] O.I. Micic, Y. Zhang, K.R. Cromack, A.D. Trifunac, M.C. Thurnauer, J. Phys. Chem. 97 (1993) 7277.